



Article

Infrared Spectroscopy as Molecular Probe of the Macroscopic Metal-Liquid Interface

Johannes Kiefer ^{1,2,3,4,*} , Johan Zetterberg ⁵ , Andreas Ehn ⁵, Jonas Evertsson ⁶, Gary Harlow ⁶ and Edvin Lundgren ⁶

¹ Technische Thermodynamik, University of Bremen, Badgasteiner Str. 1, 28359 Bremen, Germany

² School of Engineering, University of Aberdeen, Aberdeen AB24 3UE, UK

³ Erlangen Graduate School in Advanced Optical Technologies (SAOT), Universität Erlangen-Nürnberg, 91052 Erlangen, Germany

⁴ MAPEX Center for Materials and Processes, University of Bremen, Bibliothekstr. 1, 28359 Bremen, Germany

⁵ Combustion Physics, Lund University, P.O. Box 118, 221 00 Lund, Sweden;

johan.zetterberg@forbrf.lth.se (J.Z.); andreas.ehn@forbrf.lth.se (A.E.)

⁶ Division of Synchrotron Radiation Research, Lund University, 221 00 Lund, Sweden;

jonas.evertsson@sljus.lu.se (J.E.); gary.harlow@sljus.lu.se (G.H.); edvin.lundgren@sljus.lu.se (E.L.)

* Correspondence: jkiefer@uni-bremen.de; Tel.: +49-421-218-64-777

Received: 7 October 2017; Accepted: 23 November 2017; Published: 28 November 2017

Abstract: Metal-liquid interfaces are of the utmost importance in a number of scientific areas, including electrochemistry and catalysis. However, complicated analytical methods and sample preparation are usually required to study the interfacial phenomena. We propose an infrared spectroscopic approach that enables investigating the molecular interactions at the interface, but needing only minimal or no sample preparation. For this purpose, the internal reflection element (IRE) is wetted with a solution as first step. Second, a small plate of the metal of interest is put on top and pressed onto the IRE. The tiny amount of liquid that is remaining between the IRE and the metal is sufficient to produce an IR spectrum with good signal to noise ratio, from which information about molecular interactions, such as hydrogen bonding, can be deduced. Proof-of-concept experiments were carried out with aqueous salt and acid solutions and an aluminum plate.

Keywords: hydrogen bonding; ATR-FTIR; adsorption

1. Introduction

Interfaces between metals and fluids are omnipresent. Electrochemistry is the most obvious area, when an electrolyte is in contact with an electrode. This is not only the case in electrocatalysis [1,2] and energy storage devices like in a battery [3,4], but also when metals are undergoing corrosion [5,6]. Despite the importance of these systems, the analysis of the underlying physical and chemical phenomena is still a challenge. This is particularly true for those processes that are happening directly at the interface.

In a reacting system, e.g., when an electrochemical cell is under operation, an integral piece of information can be obtained by monitoring the electrical current and voltage, and/or by analyzing the bulk fluid at some distance to the surface. This allows for deducing information about the overall chemical oxidation and reduction reactions [7]. However, details about the molecular interactions at the surface are more difficult to investigate. Moreover, when the fluid (or some of its constituents) and the metal are not reacting, no information can be provided by measurements of current and bulk diagnostics.

Non-reacting metal-fluid interfaces call for surface sensitive methods. Unfortunately, the number of possible analytical techniques is rather limited. X-ray and ultraviolet radiation based methods,

such as photoelectron spectroscopy, usually require vacuum conditions and hence their application to samples containing volatile liquids is difficult [8]. Scattering and diffraction methods are usually limited to crystalline materials, and often even to atomically flat single crystal surfaces. Suitable approaches, on the other hand, can be found in the vibrational spectroscopy toolbox. Reflection-absorption infrared spectroscopy can be used to study heterogeneous catalytic processes, e.g., to identify intermediate species at the gas-solid interface [9,10]. However, its application to aqueous systems, e.g., a salt solution on a metal surface, is difficult due to the strong absorption of water in the mid-infrared.

Second-order (or even-order, in general) nonlinear effects are advantageous for studying surfaces and interfaces [11]. The even-order susceptibility is zero in the bulk of a fluid, and hence only the molecules in the optically anisotropic interfacial layer contribute to the signal, in particular when the molecules at the interface are oriented in a certain manner. In other words, the signal of even-order methods is highly surface-specific, while methods utilizing odd-order effects like infrared absorption and Raman scattering may be biased by signals from the bulk. Second-order vibrational spectroscopy can, for instance, be performed in terms of sum-frequency generation (SFG) [11,12]. However, when the IR radiation must travel through a highly absorbing medium like water, the resulting signal levels may be low. The strong absorption of water can be avoided in Raman spectroscopy because the excitation wavelength may basically be chosen arbitrarily [13], and thus it can be spectrally separated from any absorption bands. Consequently, surface-enhanced Raman scattering (SERS) can be a solution if the metal is capable of coupling with the electric field of an incident laser beam to result in the plasmonic enhancement of the inherently weak Raman signal [14]. However, the application of SERS and the data evaluation is not straightforward due to a limited reproducibility.

As a possible approach that can overcome all the above mentioned difficulties, we propose the use of attenuated total reflection infrared (ATR-IR) spectroscopy. ATR techniques are generally advantageous for studying highly absorbing media, as the radiation interacts with the sample only in an evanescent field, and hence the attenuation of the intensity is moderate [15,16]. ATR-IR has proven its potential for studying molecular phenomena at liquid-liquid and liquid-solid interfaces, including aqueous systems in the past [17–19]. However, all of the methods that are proposed to date share the disadvantage of requiring specialized equipment and/or sample preparation. For example, building an electrochemical cell on top of the spectrometer or depositing particles or a thin solid film on the ATR crystal are frequently employed approaches [20–22]. Recently, Koichumanova et al. [23] studied metal-liquid interfaces by an ATR-IR approach. They immobilized a catalyst material directly on the surface of the internal reflection element (IRE). A similar method was applied by Mundunkatowa et al. [24]. Kraack et al. [25,26] demonstrated a surface-enhanced ATR technique, utilizing gold or platinum nanoparticles at the IRE. Aguirre and co-workers [27] presented spectra from the solid-liquid interface in a specially designed microfluidic reactor. In summary, in the past, all of the work on solid-liquid interfaces using ATR-IR spectroscopy focused on adsorption directly at the IRE, adsorption at coated IREs, or adsorption to particulate matter in contact with the IRE [28].

2. Materials and Methods

The present study proposes a more straightforward technique for analyzing the liquid-solid interface. For the purpose of analyzing the molecular interactions at the interface of a metal and an aqueous solution, a modified version of the recently proposed solvent infrared spectroscopy (SIRS) method seems most suitable [18]. SIRS was developed to study the surface chemistry of nanopowders utilizing the influence of the functional groups at the particle surface on the vibrational structure of a solvent. In a typical SIRS experiment, the nanopowder was first pressed onto the internal reflection element of an ATR-IR instrument. In the second step, a solvent, such as water or an alcohol, was added to fill the void space in the fixed bed of particles. The comparison of the solvent spectrum with and without the particles yields information about the molecular interactions at and the chemistry of the surface [18].

This approach can be modified to study the molecular phenomena at a macroscopic metal-liquid interface. Figure 1 illustrates the proposed modified SIRS technique. Here, the first step is to add a droplet of the fluid onto the internal reflection element. Thereafter, the metal plate is placed on top of the fluid and pressed down by the stamp of the instrument. When the stamp is applying a force on the metal plate, most of the fluid will flow away from the IRE. Eventually, only a very thin film will remain due to the surface roughness of the metal plate. This is beneficial as there will be virtually no bulk fluid left, but the IRE will still be wetted. Consequently, the ATR-IR spectrum will carry information about the molecular interactions at the surface. As a significant advantage, the described technique requires virtually no sample preparation. This is particularly true in comparison to the approaches that are reported in the literature, which were all based on the deposition of a thin film on the IRE.

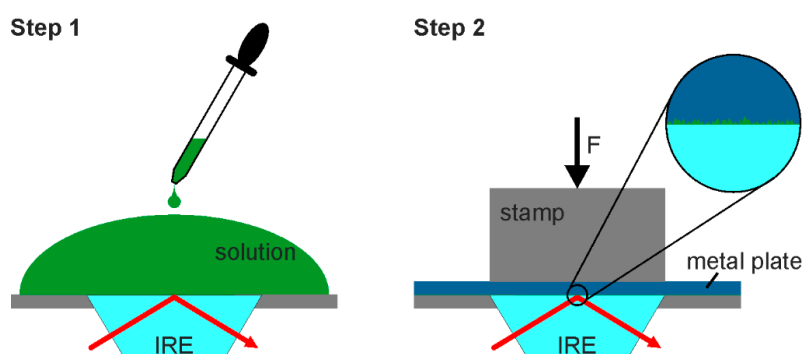


Figure 1. Schematic of the experimental procedure. IRE = internal reflection element; F = force.

As proof of the concept, experiments of three aqueous solutions (pure water, sodium sulfate solution, citric acid solution) at an aluminum surface were carried out on an Agilent Cary 630 instrument equipped with a diamond ATR unit (1 reflection, 2 cm^{-1} resolution). Deionized water ($18.2\text{ M}\Omega\text{ cm}$) was provided from a Millipore device. Aqueous solutions of 2.1 mol % Na_2SO_4 and 2.8 mol % citric acid were prepared gravimetrically.

3. Results

The pairs of spectra recorded with and without an aluminum plate are displayed in Figure 2. Note that the spectral window between 1800 and 2800 cm^{-1} does not contain any appreciable signals, and was therefore omitted. The broad and strong hydroxyl (OH) stretching band of water dominates the high wavenumber region, i.e., 2800 to 3800 cm^{-1} . This band is commonly deconvoluted into several sub-bands, indicating the different hydrogen-bonding states of water molecules [29,30]: The lower the wavenumber, the stronger the hydrogen bonding [31]. However, even with the naked eye, systematic differences between the three cases can be observed. Pure water (without Al plate) has the strongest hydrogen bonding (HB) network, as indicated by a maximum at the low wavenumber side of the band. The citric acid solution has the weakest HB network, and the sodium sulfate solution is in between the two. The fingerprint region of the spectra shows a common peak between 1630 and 1640 cm^{-1} , owing to the OH bending vibration of water. The spectrum of the sulfate solution additionally exhibits a strong S = O stretching band at 1091 cm^{-1} . The citric acid solution shows a multitude of peaks in the fingerprint region. The most dominant ones appear at 1713 and 1222 cm^{-1} , and can be assigned to the carboxylic acid groups [32].

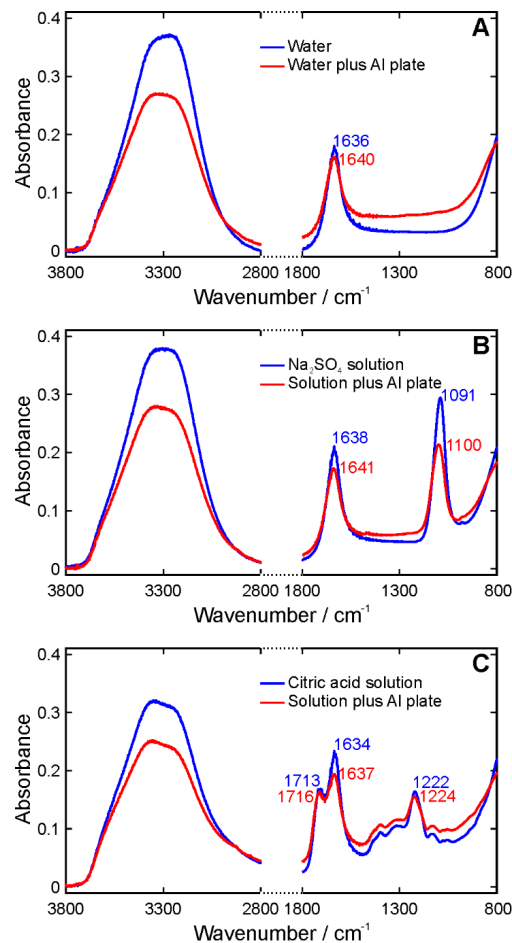


Figure 2. Fingerprint and hydroxyl (OH) stretching region of the IR spectra recorded with and without aluminum plate. (A): water; (B): aqueous sodium sulfate solution; and, (C): aqueous citric acid solution.

When the Al plate is added, all three spectra change significantly. The intensity of the OH stretching band is reduced by about 20–30%. At first glance, this reduction appears small when we argue that we move from studying the bulk fluid to the interface. However, the working principle of ATR needs to be kept in mind here. The penetration depth d_p of the evanescent field is commonly described as

$$d_p = \frac{\lambda}{2\pi \cdot n_{IRE} \cdot \left(\sin^2 \alpha - \left(\frac{n_{sample}}{n_{IRE}} \right)^2 \right)^{1/2}} \quad (1)$$

with the wavelength λ , the reflection angle α , and the refractive indices of the IRE and the sample, n_{IRE} and n_{sample} , respectively. When we assume that the liquid wets the diamond surface even in the presence of the Al plate, this penetration depth will remain the same. So, the key is to get the metal so close to the IRE surface that the probed molecules represent the thin interfacial layer. This is why a force needs to be applied to the metal plate in order to press it onto the IRE. The effective path length, on the other hand, determines the absolute absorbance, but it is an auxiliary parameter that cannot be measured. It represents the absorption path that would be necessary in a transmission experiment to observe the same attenuation of the radiation [17,33].

The shape of the OH stretching band alters such that the high-wavenumber wing becomes dominant in all three cases. Figure 3 illustrates the absorbance normalized bands and their differences in order to emphasize this effect. This change suggests a weakening of the HB network in the presence of the Al surface. The Al plate exhibits a thin oxide layer and the O^{2-} ions can act as

HB acceptors. Moreover, the Al^{3+} ions can interact with water oxygen atoms via Coulomb forces. However, the interactions at the surface are weaker than the hydrogen bonds in fully tetrahedrally coordinated bulk water. The change in the molecular interactions is further supported by the peaks in the fingerprint region. The OH bending mode slightly shifts towards higher wavenumber. The same behavior can be noted for the sulfate and the carboxylic acid peaks.

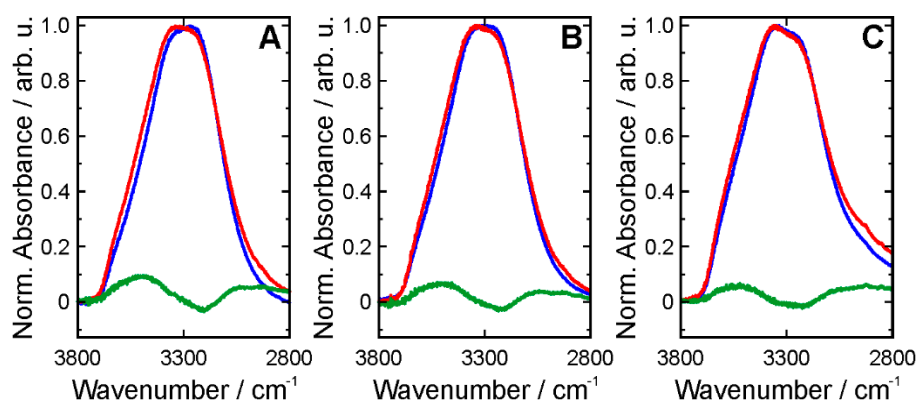


Figure 3. Normalized spectra (color code as in Figure 2) and difference spectra (green) in the OH stretching region. (A): water; (B): aqueous sodium sulfate solution; and, (C): aqueous citric acid solution.

4. Conclusions

In conclusion, we have shown that ATR-IR spectroscopy is capable of analyzing the molecular interactions between solvent molecules and a metal surface. For this purpose, the solvent or a solution was initially placed on top of the ATR crystal, and, in the second step, a metal plate was added and pressed onto the crystal. The fluid remaining in a very thin layer between the ATR crystal and the metal plate allows for recording the IR spectrum of the interfacial molecules. The IR spectrum yields information about the intermolecular interactions at the surface via monitoring of their effects on the vibrational structure of the solvent and solute. However, it needs to be kept in mind that the signals do not exclusively originate from the interfacial mono-molecular layer, but from a thin layer that is determined by the penetration depth of the ATR approach. Applying a force to the metal plate ensures that the fluid layer is thin and that the interfacial molecular interactions are sufficiently prominent in the spectra.

Using the example of water and aqueous solutions of sodium sulfate and citric acid in contact with an aluminum plate, it was shown that the presence of an Al surface results in a weakening of the hydrogen bonding network between the water molecules. A key advantage of the proposed method is its experimental simplicity and that no specialized or custom-made equipment is needed. Measurements can be performed on any ATR-IR instrument in a straightforward manner.

Author Contributions: J.Z., A.E. and E.L. initiated the project; J.K., J.E., J.Z., A.E. and E.L. conceived and designed the experiments; J.K. performed the experiments; J.K. analyzed the data; J.E., G.H. and E.L. contributed reagents/materials/analysis tools; all authors contributed to the interpretation of the data; all authors contributed to writing the paper with J.K. preparing the first draft.

Conflicts of Interest: The authors declare no conflict of interest.

References

1. Seh, Z.W.; Kibsgaard, J.; Dickens, C.F.; Chorkendorff, I.B.; Norskov, J.K.; Jaramillo, T.F. Combining theory and experiment in electrocatalysis: Insights into materials design. *Science* **2017**, *335*, 146. [[CrossRef](#)] [[PubMed](#)]
2. Stamenkovic, V.R.; Strmcnik, D.; Lopes, P.P.; Markovic, N.M. Energy and fuels from electrochemical interfaces. *Nat. Mater.* **2017**, *16*, 57–69. [[CrossRef](#)] [[PubMed](#)]

3. Wang, H.; Yang, Y.; Guo, L. Nature-Inspired Electrochemical Energy-Storage Materials and Devices. *Adv. Energy Mater.* **2017**, *7*, 1601709. [[CrossRef](#)]
4. Cho, J.; Jeong, S.; Kim, Y. Commercial and research battery technologies for electrical energy storage applications. *Prog. Energy Combust. Sci.* **2015**, *48*, 84–101. [[CrossRef](#)]
5. Manam, N.S.; Harun, W.S.W.; Shri, D.N.A.; Ghani, S.A.C.; Kurniawan, T.; Ismail, M.H.; Ibrahim, M.H.I. Study of corrosion in biocompatible metals for implants: A review. *J. Alloys Compd.* **2017**, *701*, 698–715. [[CrossRef](#)]
6. Dwivedi, D.; Lepkova, K.; Becker, T. Carbon steel corrosion: A review of key surface properties and characterization methods. *RSC Adv.* **2017**, *7*, 4580–4610. [[CrossRef](#)]
7. Zehentbauer, F.M.; Bain, E.J.; Kiefer, J. Multiple parameter monitoring in a direct methanol fuel cell. *Meas. Sci. Technol.* **2012**, *23*, 045602. [[CrossRef](#)]
8. Salmeron, M.; Schlögl, R. Ambient pressure photoelectron spectroscopy: A new tool for surface science and nanotechnology. *Surf. Sci. Rep.* **2008**, *63*, 169–199. [[CrossRef](#)]
9. Rasko, J.; Domok, A.; Baan, K.; Erdohelyi, A. FTIR and mass spectrometric study of the interaction of ethanol and ethanol-water with oxide-supported platinum catalysts. *Appl. Catal. A* **2006**, *299*, 202–211. [[CrossRef](#)]
10. McCue, A.J.; Mutch, G.A.; McNab, A.I.; Campbell, S.; Anderson, J.A. Quantitative determination of surface species and adsorption sites using Infrared spectroscopy. *Catal. Today* **2016**, *259*, 19–26. [[CrossRef](#)]
11. Kraack, J.P.; Hamm, P. Surface-sensitive and surface-specific ultrafast two-dimensional vibrational spectroscopy. *Chem. Rev.* **2017**, *117*, 10623–10664. [[CrossRef](#)] [[PubMed](#)]
12. Vidal, F.; Tadjeddine, A. Sum-frequency generation spectroscopy of interfaces. *Rep. Prog. Phys.* **2005**, *68*, 1095–1127. [[CrossRef](#)]
13. Kiefer, J. Recent advances in the characterization of gaseous and liquid fuels by vibrational spectroscopy. *Energies* **2015**, *8*, 3165–3197. [[CrossRef](#)]
14. McNay, G.; Eustace, D.; Smith, W.E.; Faulds, K.; Graham, D. Surface-Enhanced Raman Scattering (SERS) and Surface-Enhanced Resonance Raman Scattering (SERRS): A Review of Applications. *Appl. Spectrosc.* **2011**, *65*, 825–837. [[CrossRef](#)] [[PubMed](#)]
15. Chalmers, J.M.; Griffiths, P.R. *Handbook of Vibrational Spectroscopy*; John Wiley & Sons: Hoboken, NJ, USA, 2001.
16. Kiefer, J. Simultaneous acquisition of absorption and fluorescence spectra of strong absorbers utilizing an evanescent supercontinuum. *Opt. Lett.* **2016**, *41*, 5684–5687. [[CrossRef](#)] [[PubMed](#)]
17. Kiefer, J.; Frank, K.; Schuchmann, H.P. Attenuated total reflection infrared (ATR-IR) spectroscopy of a water-in-oil emulsion. *Appl. Spectrosc.* **2011**, *65*, 1024–1028. [[CrossRef](#)] [[PubMed](#)]
18. Kiefer, J.; Grabow, J.; Kurland, H.-D.; Müller, F.A. Characterization of Nanoparticles by Solvent Infrared Spectroscopy. *Anal. Chem.* **2015**, *87*, 12313–12317. [[CrossRef](#)] [[PubMed](#)]
19. Torregrosa-Coque, R.; Alvarez-Garcia, S.; Martin-Martinez, J.M. Migration of low molecular weight moiety at rubber-polyurethane interface: An ATR-IR spectroscopy study. *Int. J. Adhes. Adhes.* **2011**, *31*, 389–397. [[CrossRef](#)]
20. Wang, H.; Zhou, Y.W.; Cai, W.B. Recent applications of in situ ATR-IR spectroscopy in interfacial electrochemistry. *Curr. Opin. Electrochem.* **2017**, *1*, 73–79. [[CrossRef](#)]
21. Zandi, O.; Hamann, T.W. Determination of photoelectrochemical water oxidation intermediates on haematite electrode surfaces using operando infrared spectroscopy. *Nat. Chem.* **2016**, *8*, 778–783. [[CrossRef](#)] [[PubMed](#)]
22. Osawa, M. Dynamic process in electrochemical reactions studied by surface-enhanced infrared absorption spectroscopy (SEIRAS). *Bull. Chem. Soc. Jpn.* **1997**, *70*, 2861–2880. [[CrossRef](#)]
23. Koichumanova, K.; Visan, A.; Geerdink, B.; Lammertink, R.G.H.; Mojet, B.L.; Seshan, K.; Lefferts, L. ATR-IR spectroscopic cell for in situ studies at solid-liquid interface at elevated temperatures and pressures. *Catal. Today* **2017**, *283*, 185–194. [[CrossRef](#)]
24. Mudunkotuwa, I.A.; Al Minshid, A.; Grassian, V.H. ATR-FTIR spectroscopy as a tool to probe surface adsorption on nanoparticles at the liquid-solid interface in environmentally and biologically relevant media. *Analyst* **2014**, *139*, 870–881. [[CrossRef](#)] [[PubMed](#)]
25. Kraack, J.P.; Kaech, A.; Hamm, P. Surface Enhancement in Ultrafast 2D ATR IR Spectroscopy at the Metal-Liquid Interface. *J. Phys. Chem. C* **2016**, *120*, 3350–3359. [[CrossRef](#)]
26. Kraack, J.P.; Kaech, A.; Hamm, P. Molecule-specific interactions of diatomic adsorbates at metal-liquid interfaces. *Struct. Dyn.* **2017**, *4*, 044009. [[CrossRef](#)] [[PubMed](#)]

27. Aguirre, A.; Kler, P.A.; Berli, C.L.A.; Collins, S.E. Design and operational limits of an ATR-FTIR spectroscopic microreactor for investigating reactions at liquid-solid interface. *Chem. Eng. J.* **2014**, *243*, 197–206. [[CrossRef](#)]
28. Hind, A.R.; Bhargava, S.K.; McKinnon, A. At the solid/liquid interface: FTIR/ATR—The tool of choice. *Adv. Colloid Interface Sci.* **2001**, *93*, 91–114. [[CrossRef](#)]
29. Schmidt, D.A.; Miki, K. Structural correlations in liquid water: A new interpretation of IR spectroscopy. *J. Phys. Chem. A* **2007**, *111*, 10119–10122. [[CrossRef](#)] [[PubMed](#)]
30. Wallace, V.M.; Dhumal, N.R.; Zehentbauer, F.M.; Kim, H.J.; Kiefer, J. Revisiting the Aqueous Solutions of Dimethyl Sulfoxide by Spectroscopy in the Mid- and Near-Infrared: Experiments and Car-Parrinello Simulations. *J. Phys. Chem. B* **2015**, *119*, 14780–14789. [[CrossRef](#)] [[PubMed](#)]
31. Joseph, J.; Jemmis, E.D. Red-, blue-, or no-shift in hydrogen bonds: A unified explanation. *J. Am. Chem. Soc.* **2007**, *129*, 4620–4632. [[CrossRef](#)] [[PubMed](#)]
32. Dhumal, N.R.; Singh, M.P.; Anderson, J.A.; Kiefer, J.; Kim, H.J. Molecular interactions of a Cu-based metal-organic framework with a confined imidazolium-based ionic liquid: A combined density functional theory and experimental vibrational spectroscopy study. *J. Phys. Chem. C* **2016**, *120*, 3295–3304. [[CrossRef](#)]
33. Averett, L.A.; Griffiths, P.R. Effective path length in attenuated total reflection spectroscopy. *Anal. Chem.* **2008**, *80*, 3045–3049. [[CrossRef](#)] [[PubMed](#)]



© 2017 by the authors. Licensee MDPI, Basel, Switzerland. This article is an open access article distributed under the terms and conditions of the Creative Commons Attribution (CC BY) license (<http://creativecommons.org/licenses/by/4.0/>).